

(Ig) superfamily [3], is highly expressed in the brain and on myeloid cells, such as monocytes, macrophages, dendritic cells, and granulocytes [4, 5]. SIRP $\alpha$  seems to play an important role in the regulation of cell migration in several cell types [6] and has two known ligands – the cell surface glycoprotein CD47 and surfactant proteins A and D [7, 8]. The binding of SIRP $\alpha$  by specific antibodies, soluble CD47, or a SIRP $\alpha$ -binding CD47 peptide has been shown to inhibit neutrophil migration across epithelial monolayers or collagen-coated membranes [9, 10]. In neutrophils, SIRP $\alpha$  can be mobilized to the cell surface from intracellular storage compartments, supposedly the secondary granules, following stimulation with N-formyl-methionyl-leucyl-phenylalanine (fMLF) [9, 11]. However, the kinetics of mobilization and exact subcellular localization of SIRP $\alpha$  in neutrophils is not well understood. Therefore, here we investigated further the kinetics of mobilization, the identity of the intracellular compartment(s) from which SIRP $\alpha$  is mobilized, and its function in regulating neutrophil accumulation in inflammation *in vivo*.

## Materials and Methods

### Reagents

Polymorphprep was from Nycomed Pharma, Oslo, Norway. HRP-conjugated goat anti-mouse IgG was from Pierce, Rockford, Ill., USA. Fluorescein isothiocyanate (FITC)-conjugated anti-human CD11b (clone MEM-174) or anti-mouse CD11b (clone M1/70.15) were from ImmunoTools (Friesoythe, Germany). Dextran, Percoll and Ficoll-Paque were from Pharmacia (Uppsala, Sweden). The [<sup>57</sup>Co]vitamin B12 was supplied by Amersham Laboratories (Amersham, UK). fMLF, FITC-conjugated goat anti-mouse IgG, and other reagents were from Sigma-Aldrich, St. Louis, Mo., USA. Anti-human SIRP $\alpha$  mAbs 142, 010, 031 and 070 (all mouse IgG1) or anti-mouse SIRP $\alpha$  mAb P84 (rat IgG1) were purified from hybridoma tissue culture supernatants by ammonium sulfate precipitation and protein A or protein G chromatography (Amersham Pharmacia, Piscataway, N.J., USA) [12, 13].

### Isolation of Human Neutrophils

Experiments on human neutrophils were approved by the regional ethics committees of Umeå (2012-327-31M) or Gothenburg (543-07). Heparinized venous blood was obtained from healthy adult volunteers attending the Blood Bank at Norrlands University Hospital, Umeå, Sweden after informed consent had been given, and buffy coats were obtained from healthy blood donors through the Blood Center at the Sahlgrenska University Hospital, Gothenburg, Sweden. The study was performed in accordance with the ethical standards of the 2008 Declaration of Helsinki. Blood neutrophils were isolated (>97% purity and viability) using Polymorphprep as previously described [14]. Neutrophils for subcellular fractionation were isolated from buffy coats, using dextran sedimentation at 1 g, hypotonic lysis of the remaining erythrocytes

and centrifugation in a Ficoll-Paque gradient [15]. *In vivo* transmigrated neutrophils were collected using an experimental skin chamber approach, which is an experimental model of acute inflammation. In this model, blisters are formed by negative pressure, the blister roofs are subsequently removed, and a collection chamber filled with autologous serum is applied [16, 17]. Neutrophils were allowed to accumulate over 24 h (more than 95% neutrophils). As controls, blood neutrophils were isolated from heparinized whole blood (obtained from the same person as the one who was carrying the skin chambers) as described above. When SIRP $\alpha$  expression was analyzed on skin chamber cells, 5  $\mu$ l 7-aminoninomycin D were added to the samples before analysis, and events positive for this nuclear dye (representing necrotic/leaky cells; <5%) were excluded from further analysis.

### Subcellular Fractionation, Quantification of Granule Markers, and Preparation of Lipid Rafts

Subcellular fractionation was performed essentially according to the methods described by Borregaard et al. [18], Udby and Borregaard [19] and Dahlgren et al. [20]. In short, neutrophils isolated from buffy coats were treated with the serine protease inhibitor diisopropylfluorophosphate (8  $\mu$ M), disintegrated by nitrogen cavitation (Parr Instrument Company, Moline, Ill., USA), and the postnuclear supernatant was centrifuged either on a three-layer Percoll gradient (to isolate the specific and gelatinase granules separately) or on a flotation gradient (to isolate the secretory vesicles from the plasma membranes). The gradients were collected in 1.5- or 1-ml fractions, respectively, by aspiration from the bottom of the centrifuge tube, and the localization of subcellular organelles in the gradients was determined by quantifying vitamin B12-binding protein (marker for the specific granules) with the cyanocobalamin technique, by quantifying gelatinase (marker for the gelatinase granules) and myeloperoxidase (marker for the azurophil granules) using ELISA methods, or alkaline phosphatase (marker for secretory vesicles and plasma membranes) measured as hydrolysis of *p*-nitrophenyl phosphate (2 mg/ml) in the presence or absence of Triton X-100 (0.4%). Lipid rafts or detergent-resistant membranes were isolated from neutrophil membranes as previously described [21]. The presence of SIRP $\alpha$  or the lipid raft marker stomatin in neutrophil subcellular fractions was determined by Western blot analysis as previously described [21, 22].

### Mice and Isolation of Murine Neutrophils

Male and female SIRP $\alpha$ -mutant mice, which lack most of the SIRP $\alpha$  cytoplasmic domain, were previously described [23, 24]. SIRP $\alpha$ -mutant mice and their homozygous wild-type littermates were kept in accordance with local guidelines and maintained in a specific pathogen-free barrier facility. The experiments were performed in compliance with relevant Swedish and institutional laws and guidelines and approved by the Umeå research animal ethics committee (A14-12). Bone marrow neutrophils were isolated from femurs of 2- to 4-month-old mice, using a Percoll gradient as previously described [25] and were resuspended at  $5 \times 10^6$ /ml in cold HBSS containing Ca<sup>2+</sup> and Mg<sup>2+</sup> (HBSS<sup>++</sup>). These preparations routinely contained more than 85% neutrophils.

### Murine Uric Acid-Induced Peritonitis

Peritonitis was induced by injecting 200  $\mu$ l 10% (wt/vol) uric acid in saline as previously described [26]. At the indicated time points, the peritoneal cavity was lavaged with 5 ml PBS + 2% FCS.

The total number of cells in the lavages was determined, using Türk's reagent and a Bürker chamber, and the percentage of neutrophils was determined in cytospin preparations stained with May-Grünwald/Giemsa.

#### *fMLF-Induced Receptor Expression and FACS Analysis*

Neutrophils ( $2.5 \times 10^5$ ) in a volume of 500  $\mu$ l HBSS<sup>++</sup> with 0.25% HSA were incubated at 37°C in the presence or absence of fMLF or TNF $\alpha$  for the times indicated. In some experiments, neutrophils were preincubated for 15 min with inhibitors, followed by incubation in the presence or absence of fMLF for 20 min. Cells were then washed in ice-cold PBS and resuspended in ice-cold staining buffer (RPMI 1640 with 2% FCS and 1 mg/ml human IgG) with the indicated mAbs and incubated for 30 min on ice. If appropriate, cells were also incubated for 30 min on ice in the dark with FITC-conjugated goat anti-mouse IgG. The cells were finally washed, resuspended in cold PBS/1% BSA and analyzed by flow cytometry (FACScan or FACSCalibur, Becton Dickinson) and CellQuest software (Becton Dickinson).

#### *Statistics*

Statistical analyses were performed by one-parameter ANOVA and Tukey's post hoc test, or Student's t test for unpaired comparisons. All results are expressed as mean  $\pm$  SEM.

## **Results and Discussion**

### *Increased Neutrophil Cell Surface SIRP $\alpha$ Expression following Inflammatory Transmigration in vivo and following Inflammatory Activation in vitro*

Due to their vast amount of granules, each containing a large array of membrane proteins, neutrophil activation and degranulation rapidly increase the cell surface levels of many proteins to reflect the shifting functional need of these cells [27]. The accumulation of neutrophils in human skin chamber exudates represents an aseptic model of inflammation to study in vivo activated neutrophils that have transmigrated from the blood into a skin chamber containing autologous serum factors, primarily C5a and IL-8 [17]. A large fraction of such neutrophils had higher levels of SIRP $\alpha$  on their cell surface as compared to peripheral blood neutrophils isolated from the same individual (fig. 1a). The population of exudate neutrophils with a reduced SIRP $\alpha$  expression in these experiments was proportional to the amount of apoptotic cells (data not shown), which is in line with our recent finding that SIRP $\alpha$  expression is downregulated during neutrophil apoptosis [13]. The bacterial chemotactic peptide fMLF can also induce mobilization of membrane proteins from intracellular granules to the neutrophil cell surface in vitro [22, 28]. We found that SIRP $\alpha$  was dose- and time-dependently increased by fMLF in human neutrophils in vitro (fig. 1b), a response evenly distributed with-

in the neutrophil population (fig. 1c). Since fMLF-stimulated neutrophil degranulation has been suggested to involve signaling by members of the mitogen-activated protein kinase (MAPK) family [29], we investigated whether fMLF-induced SIRP $\alpha$  upregulation was affected by specific inhibitors of p38 MAPK or ERK. The p38 MAPK inhibitor SB203580, but not the ERK inhibitor PD98059, used at concentrations shown to inhibit Fc $\gamma$ R-mediated phagocytosis [30], had an inhibitory effect on fMLF-induced cell surface SIRP $\alpha$  expression (fig. 1d). Thus, these data are in line with the finding that degranulation of secondary granules is partly mediated by p38 MAPK but not by ERK [29]. In exudate neutrophils, it is unclear whether SIRP $\alpha$  is upregulated as a result of early activation during transendothelial migration or as a gradual response to increasing concentrations of chemotactic factors after completing the transmigration process. The latter hypothesis is supported by our in vitro data, showing that neutrophil SIRP $\alpha$  is upregulated dose-dependently by fMLF with rather modest effects observed at the lower chemoattractant concentrations that would be involved in initial neutrophil chemotactic recruitment from the blood in vivo (fig. 1b).

### *Subcellular Localization of SIRP $\alpha$ in Human Neutrophils*

To get a detailed understanding of the intracellular localization of SIRP $\alpha$ , we investigated subcellular neutrophil fractions using immunoblot analysis and correlated the presence of SIRP $\alpha$  in these fractions with specific markers for azurophil granules (myeloperoxidase), specific granules (vitamin B12-binding protein), gelatinase granules (gelatinase but no vitamin B12-binding protein), and secretory vesicles/plasma membrane (latent/nonlatent alkaline phosphatase, respectively). Using a three-step Percoll gradient, allowing for separation of the specific granules from the gelatinase granules, we found that SIRP $\alpha$  colocalized with markers for specific granules, gelatinase granules, as well as light membranes (secretory vesicles/plasma membrane; fig. 2a). However, we could not detect SIRP $\alpha$  in azurophil granules (fig. 2a). Using a flotation gradient, where secretory vesicles are separated from the plasma membrane in the upper part of the gradient, we could separately confirm the presence of SIRP $\alpha$  in both the secretory vesicles and the plasma membrane (fig. 2b). Proteins of importance for signaling over the cell membrane have been shown to be often associated with so-called lipid rafts or detergent-resistant membrane domains. We explored the possibility that SIRP $\alpha$  is localized in such domains in neutrophils, knowing that these cells contain lipid rafts not

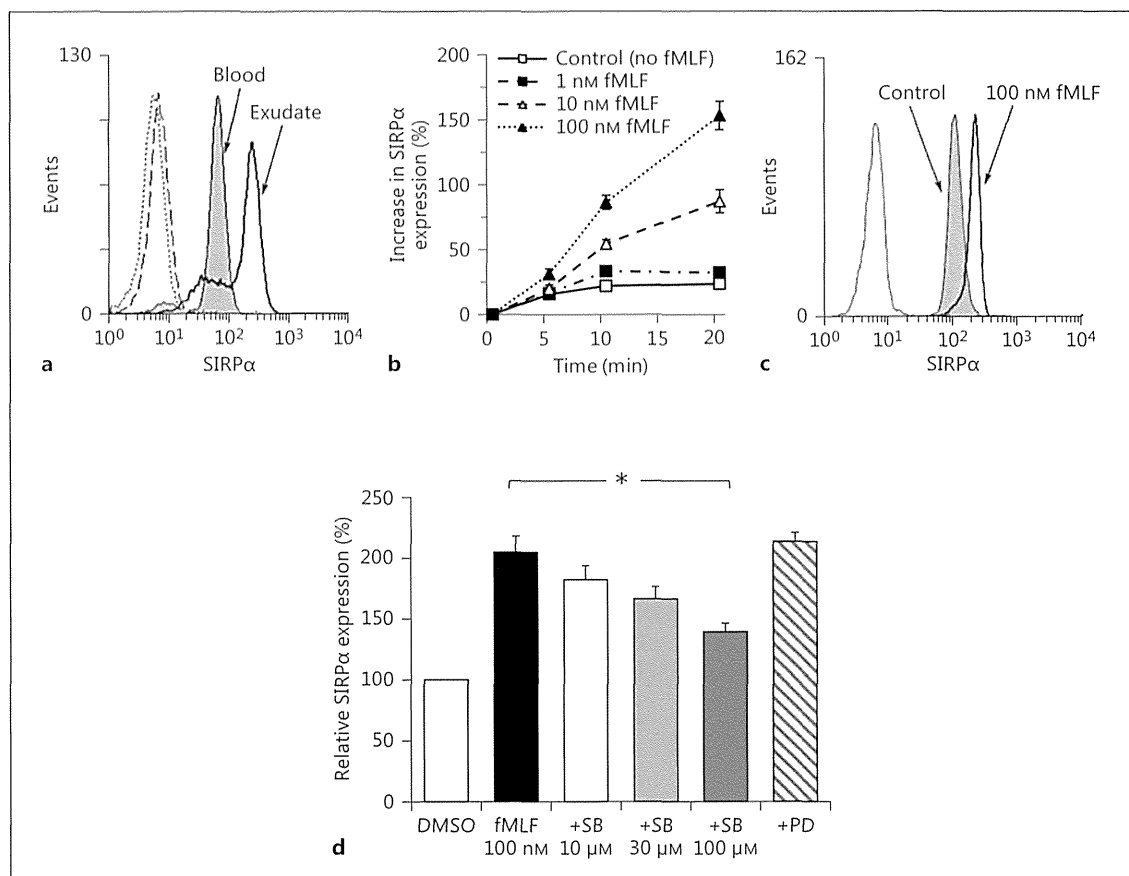


**Fig. 1.** Neutrophil cell surface SIRP $\alpha$  expression is increased following in vivo transmigration or stimulation with fMLF in vitro. **a** Cell surface SIRP $\alpha$  expression was increased on human skin chamber exudate neutrophils (bold line) as compared to that on peripheral blood neutrophils (grey histogram). The fluorescence intensity of exudate neutrophils (dotted line) or peripheral blood neutrophils from the same donor (dashed line) incubated with control IgG is also shown. The data are representative of 3 separate experiments with virtually identical results. **b** Dose- and time-dependent upregulation of SIRP $\alpha$  on human neutrophils following incubation for 5–20 min at 37°C in the absence or presence of 1–100 nM fMLF. Values are means  $\pm$  SEM for 3 separate experiments. **c** Flow-cytometric profiles of SIRP $\alpha$  expression in unstim-

ulated human neutrophils (grey histogram, control) or following incubation for 20 min at 37°C with 100 nM fMLF (bold line). The thin line indicates cells labeled with an isotype control antibody. Data from 1 representative experiment presented in **b** are shown. **d** Neutrophils were preincubated for 15 min with the inhibitors SB203580 (SB; p38 MAPK inhibitor) or 50  $\mu$ M PD98059 (PD; ERK inhibitor) followed by incubation in the presence of 100 nM fMLF for 15 min at 37°C. Cells were then labeled with anti-SIRP $\alpha$  mAb and analyzed by flow cytometry. Neutrophil SIRP $\alpha$  expression was calculated as percent of that in neutrophils incubated only in vehicle (DMSO). Values are means  $\pm$  SEM of 3–5 separate experiments. \*  $p < 0.05$ , one-parameter ANOVA and Tukey's post hoc test.

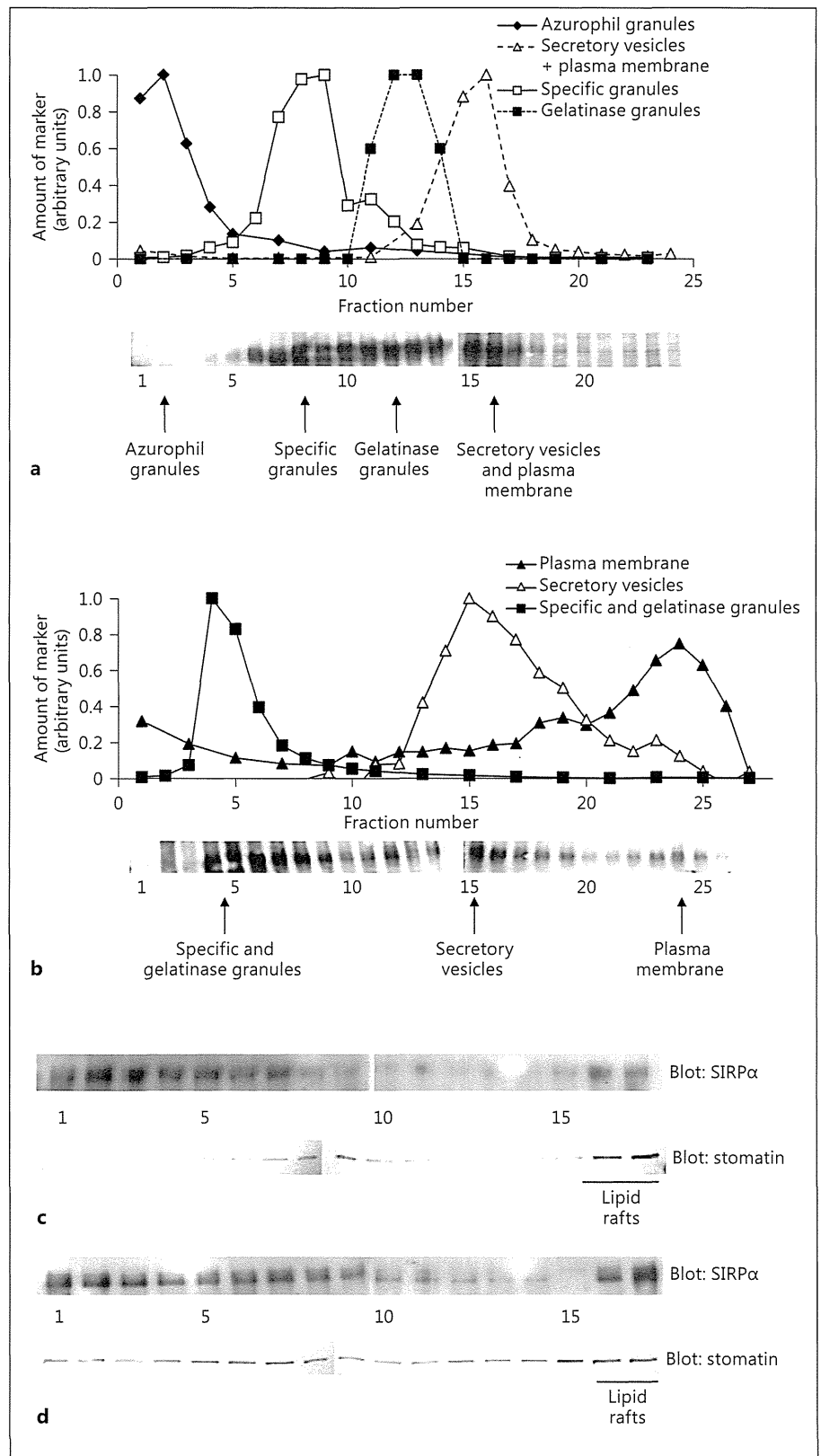
only in the plasma membrane but also in intracellular granule membranes [21]. Detergent-resistant fractions were isolated from the light membrane fraction of neutrophils (secretory vesicles/plasma membranes), as well as from the specific and gelatinase granule membranes, by flotation in a Percoll gradient. In both these compartments, SIRP $\alpha$  was to some extent present in the lipid rafts (fig. 2c, d), colocalizing with the raft marker stomatin (fig. 2c, d). Thus, our data confirmed the presence of SIRP $\alpha$

in neutrophil-specific granules as suggested previously [11], but could in addition show SIRP $\alpha$  to be present in the gelatinase granules and the secretory vesicles.

#### *SIRP $\alpha$ Mediates Negative Fine-Tuning of Neutrophil Accumulation in Inflammation*

The functional significance of a gradually increased SIRP $\alpha$  expression in relation to neutrophil migration is not entirely clear. However, ligation of SIRP $\alpha$ , either by

**Fig. 2.** Subcellular localization of SIRP $\alpha$  in neutrophils. Human neutrophils were fractionated on a three-step gradient (a) or a flotation gradient (b) as described in Materials and Methods. The localization of neutrophil granules in the gradient was determined by marker analysis of the fractions; arrows indicate peak fractions of the different markers. Isolated membranes from plasma membrane/secretory vesicles (c) or specific/gelatinase granules (d) were resuspended in relaxation buffer containing Triton X-100, layered under Percoll and centrifuged as described in Materials and Methods. The collected fractions were analyzed for stomatin (lipid raft marker) by immunoblotting and the results show that Triton-insoluble membrane domains have floated upwards to gradient fractions 16 and 17. The localization of SIRP $\alpha$  in the fractions is shown by immunoblotting, using a combination of mAbs 010, 031, and 070.



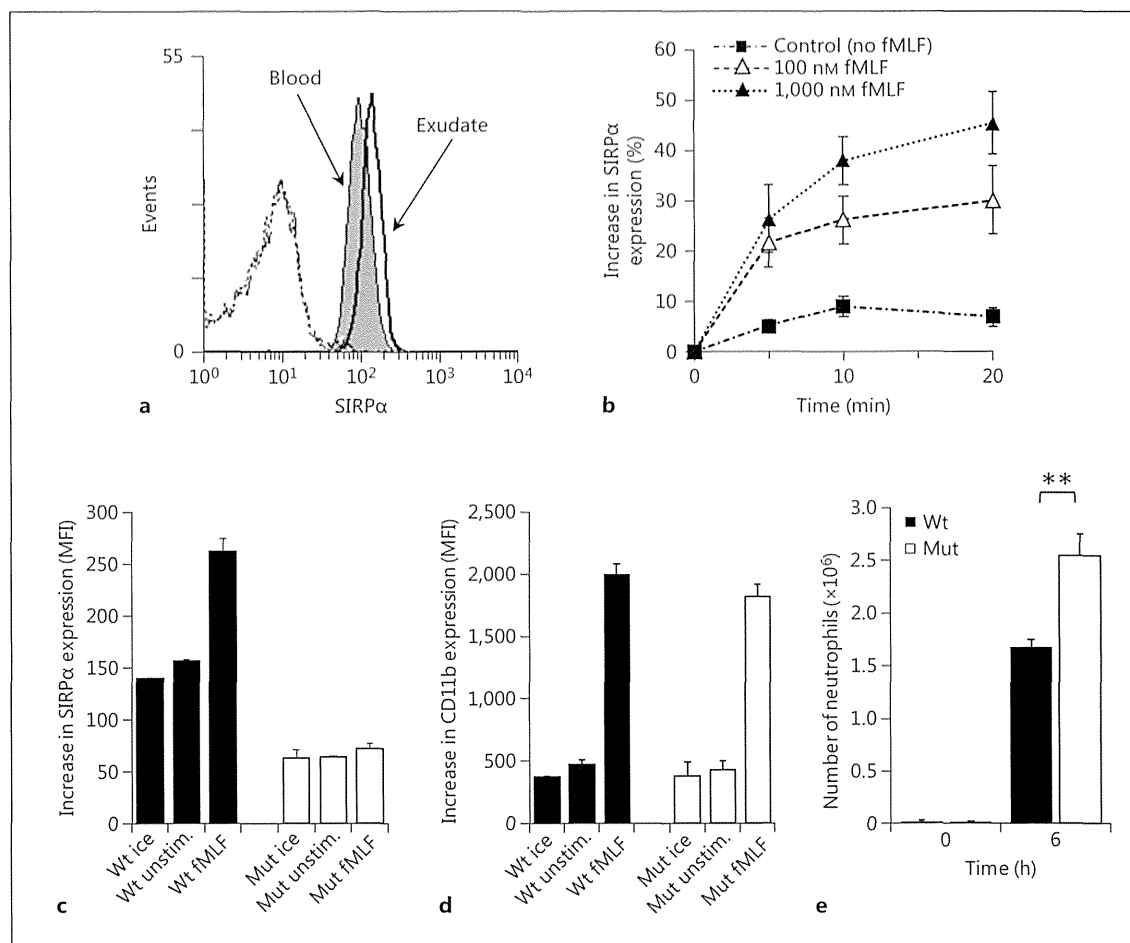


**Fig. 3.** Lack of SIRP $\alpha$  signaling and its upregulation to the cell surface enhance neutrophil accumulation in inflammation. **a** Increased expression of SIRP $\alpha$  by peritoneal exudate neutrophils in wild-type mice following injection of uric acid (bold line) as compared with that on murine peripheral blood neutrophils (grey histogram). The data are representative of 3 separate mice showing virtually identical results. **b** Dose- and time-dependent upregulation of SIRP $\alpha$  on murine neutrophils following incubation for 5–20 min at 37°C in the absence or presence of fMLF. The data are expressed as a percent increase from the SIRP $\alpha$  expression on cells kept on ice (0 min). Values are means  $\pm$  SEM of 3 separate experiments. **c** Neutrophil SIRP $\alpha$  expression in wild-type or SIRP $\alpha$  mutant neutrophils, either kept on ice or incubated for 20 min at 37°C

in the absence or presence of 1,000 nM fMLF. Data are means  $\pm$  SEM of 4 separate mice per genotype. **d** Neutrophil CD11b expression in wild-type or SIRP $\alpha$  mutant neutrophils, either kept on ice or incubated for 20 min at 37°C in the absence or presence of 1,000 nM fMLF. Data are means  $\pm$  SEM of 4 separate mice per genotype. **e** Wild-type or SIRP $\alpha$ -mutant mice were injected i.p. with 10% uric acid, and peritoneal cells were harvested 6 h later. The total number of cells was determined using a Bürker chamber, and the fraction of neutrophils was determined from cytospin preparations stained with May-Grünwald-Giemsa. Data represent means  $\pm$  SEM of 5 mice per group. \*\*  $p < 0.01$ , using Student's *t* test for unpaired comparisons. MFI = Mean fluorescence intensity; Wt = wild-type; Mut = mutant; unstim. = unstimulated.

antibodies, by a soluble form of its ligand CD47, or by using a CD47-derived peptide, was reported to inhibit neutrophil migration across epithelial cells or cell-free collagen-coated filters *in vitro* [9, 10]. This suggests an active role played by SIRP $\alpha$  in negatively regulating neutrophil migration. To investigate this further, we studied SIRP $\alpha$ -mutant mice, which only express the extracellular do-

main of SIRP $\alpha$ , while the cytoplasmic signaling ITIM domain is deleted [23]. Similar to that in human exudate neutrophils, we found that SIRP $\alpha$  was upregulated on the surface of wild-type neutrophils accumulating in urate-induced peritonitis (fig. 3a) or when stimulated with fMLF *in vitro* (fig. 3b). However, in SIRP $\alpha$ -mutant neutrophils, we found a more than 50% reduction in the

amount of the SIRP $\alpha$  extracellular domain on the cell surface of nonstimulated cells as compared with wild-type neutrophils (fig. 3c). In addition, mutant cells were unable to upregulate SIRP $\alpha$  on the cell surface in response to fMLF (fig. 3c). It was unlikely that this was a result of defects in degranulation, since CD11b was found to be upregulated normally in mutant neutrophils stimulated with fMLF (fig. 3d). The fact that SIRP $\alpha$  can neither signal nor be increased on the cell surface in response to inflammatory activation in SIRP $\alpha$ -mutant neutrophils suggested that these mice would represent a good model to investigate a functional role of SIRP $\alpha$  in vivo. For this, we used the uric acid-induced peritonitis model of sterile inflammation, in which acute neutrophil influx into the peritoneal cavity is mediated by IL-1 $\beta$ , IL-6, and TNF $\alpha$  produced by resident peritoneal macrophages [31]. In addition, a role for macrophage inflammatory protein-2 and peritoneal mast cells has also been suggested in this model [32]. We found that significantly more neutrophils were recovered in peritoneal lavages from SIRP $\alpha$ -mutant mice, as compared with that in wild-type controls at 6 h after uric acid injection ( $p < 0.01$ ; fig. 3e). This was neither the result of an increased number of peritoneal neutrophils in naïve SIRP $\alpha$ -mutant mice (0 h; fig. 3e) nor the result of increased numbers of circulating neutrophils, since wild-type and mutant mice had similar numbers of neutrophils in blood ( $795 \pm 70$  vs.  $723 \pm 112$  cells/ $\mu$ l, respectively;  $p > 0.05$ ). These data therefore suggest that an increased level of SIRP $\alpha$  on the neutrophil cell surface could serve to negatively fine-tune neutrophil accumulation at sites of inflammation. While preparing this manuscript, Zen et al. [33] presented data confirming our findings by showing that SIRP $\alpha$ -mutant mice have an in-

creased accumulation of neutrophils in a model of zymosan-induced peritonitis. Since CD47 can function as a ligand for SIRP $\alpha$  [34] and CD47 is expressed by virtually all cells in the host [35], the ability of SIRP $\alpha$  to negatively fine-tune neutrophil accumulation in inflammation is possibly mediated by the interaction between neutrophil SIRP $\alpha$  and CD47 on other cells.

In conclusion, we have shown that SIRP $\alpha$  is rapidly mobilized to the cell surface from neutrophil secretory vesicles, gelatinase granules, and specific granules, following stimulation with fMLF in vitro or in vivo transmigration into tissue. The enhanced accumulation during inflammation in vivo of murine neutrophils lacking both the signaling SIRP $\alpha$  ITIM domain and the ability to increase the level of the SIRP $\alpha$  extracellular domain in response to inflammation suggests that SIRP $\alpha$  negatively fine-tunes the accumulation of inflammatory-activated neutrophils.

### Acknowledgements

This study was supported by grants from the Swedish Research Council (2012-2702; P.-A.O.: 2011-3358; A.K.: 16X-20247; J.B.), the King Gustaf V 80-Year Foundation (A.K., J.B., and P.-A.O.), the Göteborg Rheumatism Association (A.K. and J.B.), the Swedish state under the LUA/ALF agreement (A.K. and J.B.), the Faculty of Medicine, Umeå University, and a Young Researcher Award from Umeå University (P.-A.O.). We thank Ms. Barbro Borgström for excellent technical assistance.

### Disclosure Statement

The authors declare no competing financial interests.

### References

- ▶ 1 Witko-Sarsat V, Rieu P, Descamps-Latscha B, Lesavre P, Halbwachs-Mecarelli L: Neutrophils: molecules, functions and pathophysiological aspects. *Lab Invest* 2000;80:617–653.
- ▶ 2 Borregaard N: Neutrophils, from marrow to microbes. *Immunity* 2010;33:657–670.
- ▶ 3 Kharitonov A, Chen Z, Sures I, Wang H, Schilling J, Ullrich A: A family of proteins that inhibit signalling through tyrosine kinase receptors. *Nature* 1997;386:181–186.
- ▶ 4 Adams S, van der Laan LJ, Vernon-Wilson E, Renardel DL, Dopp EA, Dijkstra CD, Simmons DL, van den Berg TK: Signal-regulatory protein is selectively expressed by myeloid and neuronal cells. *J Immunol* 1998;161:1853–1859.
- ▶ 5 Seiffert M, Cant C, Chen Z, Rappold I, Brugerger W, Kanz L, Brown EJ, Ullrich A, Bühring H-J: Human signal-regulatory protein is expressed on normal, but not on subsets of leukemic myeloid cells and mediates cellular adhesion involving its counterreceptor CD47. *Blood* 1999;94:3633–3643.
- ▶ 6 Oshima K, Ruhul Amin AR, Suzuki A, Hamaguchi M, Matsuda S: SHPS-1, a multifunctional transmembrane glycoprotein. *FEBS Lett* 2002;519:1–7.
- ▶ 7 Gardai SJ, Xiao YQ, Dickinson M, Nick JA, Voelker DR, Greene KE, Henson PM: By binding SIRP $\alpha$  or calreticulin/CD91, lung collectins act as dual function surveillance molecules to suppress or enhance inflammation. *Cell* 2003;115:13–23.
- ▶ 8 Oldenborg P-A: CD47: a cell surface glycoprotein which regulates multiple functions of hematopoietic cells in health and disease. *ISRN Hematol* 2013;2013:614619.
- ▶ 9 Liu Y, Bühring H-J, Zen K, Burst SL, Schnell FJ, Williams IR, Parkos CA: Signal regulatory protein (SIRP $\alpha$ ), a cellular ligand for CD47, regulates neutrophil transmigration. *J Biol Chem* 2002;277:10028–10036.
- ▶ 10 Liu Y, O'Connor MB, Mandell KJ, Zen K, Ullrich A, Bühring HJ, Parkos CA: Peptide-mediated inhibition of neutrophil transmigration by blocking CD47 interactions with signal regulatory protein alpha. *J Immunol* 2004;172:2578–2585.

- ▶11 Liu Y, Soto I, Tong Q, Chin A, Buhning HJ, Wu T, Zen K, Parkos CA: SIRPbeta1 is expressed as a disulfide-linked homodimer in leukocytes and positively regulates neutrophil transepithelial migration. *J Biol Chem* 2005; 280:36132–36140.
- ▶12 Latour S, Tanaka H, Demeure C, Mateo V, Rubio M, Brown EJ, Maliszewski C, Lindberg FP, Oldenborg A, Ullrich A, Delespesse G, Sarfati M: Bidirectional negative regulation of human T and dendritic cells by CD47 and its cognate receptor signal-regulator protein-alpha: down-regulation of IL-12 responsiveness and inhibition of dendritic cell activation. *J Immunol* 2001;167:2547–2554.
- ▶13 Stenberg Å, Sehlin J, Oldenborg PA: Neutrophil apoptosis is associated with loss of signal regulatory protein alpha (SIRPα) from the cell surface. *J Leukoc Biol* 2013;93:403–412.
- ▶14 Oldenborg P-A, Sehlin J: Hyperglycemia in vitro attenuates insulin-stimulated chemokinesis in normal human neutrophils. Role of protein kinase C activation. *J Leuk Biol* 1999; 65:635–640.
- ▶15 Böyum A: Separation of leukocytes from blood and bone marrow. *Scand J Clin Lab Invest* 1968;21:77–89.
- ▶16 Christenson K, Björkman L, Karlsson J, Sundqvist M, Movitz C, Speert DP, Dahlgren C, Bylund J: In vivo-transmigrated human neutrophils are resistant to antiapoptotic stimulation. *J Leukoc Biol* 2011;90:1055–1063.
- ▶17 Follin P: Skin chamber technique for study of in vivo exudated human neutrophils. *J Immunol Methods* 1999;232:55–65.
- ▶18 Borregaard N, Heiple JM, Simons ER, Clark RA: Subcellular localization of the b-cytochrome component of the human neutrophil microbicidal oxidase: translocation during activation. *J Cell Biol* 1983;97:52–61.
- ▶19 Udby L, Borregaard N: Subcellular fractionation of human neutrophils and analysis of subcellular markers. *Methods Mol Biol* 2007; 412:35–56.
- ▶20 Dahlgren C, Carlsson SR, Karlsson A, Lundqvist H, Sjölin C: The lysosomal membrane glycoproteins Lamp-1 and Lamp-2 are present in mobilizable organelles, but are absent from the azurophil granules of human neutrophils. *Biochem J* 1995;311:667–674.
- ▶21 Feuk-Lagerstedt E, Samuelsson M, Mosgoeller W, Movitz C, Rosqvist A, Bergström J, Larsson T, Steiner M, Prohaska R, Karlsson A: The presence of stomatin in detergent-insoluble domains of neutrophil granule membranes. *J Leuk Biol* 2002;72:970–977.
- ▶22 Karlsson A, Follin P, Leffler H, Dahlgren C: Galectin-3 activates the NADPH-oxidase in exudated but not peripheral blood neutrophils. *Blood* 1998;91:3430–3438.
- ▶23 Inagaki K, Yamao T, Noguchi T, Matozaki T, Fukunaga K, Takada T, Hosooka T, Akira S, Kasuga M: SHPS-1 regulates integrin-mediated cytoskeletal reorganization and cell motility. *EMBO J* 2000;19:6721–6731.
- ▶24 Okazawa H, Motegi S, Ohyama N, Ohnishi H, Tomizawa T, Kaneko Y, Oldenborg P-A, Ishikawa O, Matozaki T: Negative regulation of phagocytosis in macrophages by the CD47-SHPS-1 system. *J Immunol* 2005;174:2004–2011.
- ▶25 Lowell CA, Fumagalli L, Berton G: Deficiency of Src family kinases p59/61hck and p58c-fgr results in defective adhesion-dependent neutrophil functions. *J Cell Biol* 1996;133:895–910.
- ▶26 Itou T, Collins LV, Thorén FB, Dahlgren C, Karlsson A: Changes in activation states of murine polymorphonuclear leukocytes (PMN) during inflammation: a comparison of bone marrow and peritoneal exudate PMN. *Clin Vaccine Immunol* 2006;13:575–583.
- ▶27 Faurschou M, Borregaard N: Neutrophil granules and secretory vesicles in inflammation. *Microbes Infect* 2003;5:1317–1327.
- ▶28 Karlsson A: Wheat germ agglutinin induces NADPH-oxidase activity in human neutrophils by interaction with mobilizable receptors. *Infect Immun* 1999;67:3461–3468.
- ▶29 Mocsai A, Jakus Z, Vantus T, Berton G, Lowell CA, Ligeti E: Kinase pathways in chemoattractant-induced degranulation of neutrophils: the role of p38 mitogen-activated protein kinase activated by Src family kinases. *J Immunol* 2000;164:4321–4331.
- ▶30 Olsson M, Oldenborg P-A: CD47 on experimentally senescent murine RBCs inhibits phagocytosis following Fcγ receptor-mediated but not scavenger receptor-mediated recognition by macrophages. *Blood* 2008;112: 4259–4267.
- ▶31 Martin WJ, Walton M, Harper J: Resident macrophages initiating and driving inflammation in a monosodium urate monohydrate crystal-induced murine peritoneal model of acute gout. *Arthritis Rheum* 2009;60:281–289.
- ▶32 Mercer-Jones MA, Shrotri MS, Heinzelmann M, Peyton JC, Cheadle WG: Regulation of early peritoneal neutrophil migration by macrophage inflammatory protein-2 and mast cells in experimental peritonitis. *J Leukoc Biol* 1999;65:249–255.
- ▶33 Zen K, Guo Y, Bian Z, Lv Z, Zhu D, Ohnishi H, Matozaki T, Liu Y: Inflammation-induced proteolytic processing of the SIRPα cytoplasmic ITIM in neutrophils propagates a proinflammatory state. *Nat Commun* 2013;4:2436.
- ▶34 Jiang P, Lagenaur CF, Narayanan V: Integrin-associated protein is a ligand for the P84 neural adhesion molecule. *J Biol Chem* 1999;274: 559–562.
- ▶35 Reinhold MI, Lindberg FP, Plas D, Reynolds S, Peters MG, Brown EJ: In vivo expression of alternatively spliced forms of integrin-associated protein (CD47). *J Cell Sci* 1995;108: 3419–3425.

# Role of the Protein Tyrosine Phosphatase Shp2 in Homeostasis of the Intestinal Epithelium

Hironori Yamashita<sup>1,2</sup>, Takenori Kotani<sup>1\*</sup>, Jung-ha Park<sup>1</sup>, Yoji Murata<sup>1</sup>, Hideki Okazawa<sup>1</sup>, Hiroshi Ohnishi<sup>3</sup>, Yonson Ku<sup>2</sup>, Takashi Matozaki<sup>1,4\*</sup>

**1** Division of Molecular and Cellular Signaling, Department of Biochemistry and Molecular Biology, Kobe University Graduate School of Medicine, Kobe, Hyogo, Japan, **2** Division of Hepato-Biliary-Pancreatic Surgery, Department of Surgery, Kobe University Graduate School of Medicine, Kobe, Hyogo, Japan, **3** Department of Laboratory Sciences, Gunma University Graduate School of Health Sciences, Maebashi, Gunma, Japan, **4** Laboratory of Biosignal Sciences, Institute for Molecular and Cellular Regulation, Gunma University, Maebashi, Gunma, Japan

## Abstract

Protein tyrosine phosphorylation is thought to be important for regulation of the proliferation, differentiation, and rapid turnover of intestinal epithelial cells (IECs). The role of protein tyrosine phosphatases in such homeostatic regulation of IECs has remained largely unknown, however. Src homology 2-containing protein tyrosine phosphatase (Shp2) is a ubiquitously expressed cytoplasmic protein tyrosine phosphatase that functions as a positive regulator of the Ras–mitogen-activated protein kinase (MAPK) signaling pathway operative downstream of the receptors for various growth factors and cytokines, and it is thereby thought to contribute to the regulation of cell proliferation and differentiation. We now show that mice lacking Shp2 specifically in IECs (Shp2 CKO mice) develop severe colitis and die as early as 3 to 4 weeks after birth. The number of goblet cells in both the small intestine and colon of Shp2 CKO mice was markedly reduced compared with that for control mice. Furthermore, Shp2 CKO mice showed marked impairment of both IEC migration along the crypt-villus axis in the small intestine and the development of intestinal organoids from isolated crypts. The colitis as well as the reduction in the number of goblet cells apparent in Shp2 CKO mice were normalized by expression of an activated form of K-Ras in IECs. Our results thus suggest that Shp2 regulates IEC homeostasis through activation of Ras and thereby protects against the development of colitis.

**Citation:** Yamashita H, Kotani T, Park J-h, Murata Y, Okazawa H, et al. (2014) Role of the Protein Tyrosine Phosphatase Shp2 in Homeostasis of the Intestinal Epithelium. PLoS ONE 9(3): e92904. doi:10.1371/journal.pone.0092904

**Editor:** Reiko Sugiura, Kinki University School of Pharmaceutical Sciences, Japan

**Received:** December 29, 2013; **Accepted:** February 26, 2014; **Published:** March 27, 2014

**Copyright:** © 2014 Yamashita et al. This is an open-access article distributed under the terms of the Creative Commons Attribution License, which permits unrestricted use, distribution, and reproduction in any medium, provided the original author and source are credited.

**Funding:** This work was supported by a Grant-in-Aid for Scientific Research (B) (23370061) and a Grant-in-Aid for Scientific Research on Innovative Area (25114709) from the Ministry of Education, Culture, Sports, Science, and Technology of Japan (<http://www.mext.go.jp/english/>). The funders had no role in study design, data collection and analysis, decision to publish, or preparation of the manuscript.

**Competing Interests:** The authors have declared that no competing interests exist.

\* E-mail: matozaki@med.kobe-u.ac.jp (TM); kotani@med.kobe-u.ac.jp (TK)

## Introduction

Intestinal epithelial cells (IECs) play a central role in the absorption of nutrients and water by the intestine as well as contribute to protection against ingested pathogens by providing a functional barrier. In mammals, IECs of the small and large intestine are regenerated continuously from stem cells throughout adulthood [1]. The stem cells that give rise to IECs reside in a region near the base of intestinal crypts. These stem cells generate proliferating progeny, known as transient amplifying (TA) cells, that migrate out of the stem cell niche, cease to proliferate, and initiate differentiation into the various cell lineages of mature intestinal villi, including absorptive enterocytes, mucin-secreting goblet cells, peptide hormone-secreting neuroendocrine cells, and antimicrobial peptide-producing Paneth cells [2]. Cells of the first three of these four lineages mature and migrate up the crypt toward the tip of intestinal villi, whereas Paneth cells travel down to the base of the crypt. Absorptive enterocytes in particular have a short life span, being released into the gut lumen after they have migrated to the tip of the villi. Such elimination of IECs is thought to be triggered by either spontaneous apoptosis [3] or overcrowding [4] of IECs, although the mechanism by which the precise timing of elimination is determined remains poorly understood.

The continuous production of new IECs from each crypt is thus balanced by the elimination of older cells at the luminal side of the intestine, resulting in a rapid turnover of IECs (4 to 5 days in the mouse) [1,2].

Protein tyrosine phosphorylation is an important signaling mechanism that regulates the proliferation, differentiation, migration, and survival of IECs. For instance, epidermal growth factor (EGF), whose receptor is a protein tyrosine kinase (PTK), is thought to be essential for IEC proliferation [5]. In addition, ephrins and their PTK receptors are implicated in the proliferation of intestinal stem cells and the positioning of IECs along the crypt-villus axis [1,6,7]. In contrast to PTKs, the importance of protein tyrosine phosphatases (PTPs) in the regulation of IECs has remained largely unknown, with the exception that stomach cancer-associated protein tyrosine phosphatase-1 (SAP-1, also known as PTPRH), a receptor-type PTP, is specifically expressed in IECs [8] and might play a role in control of the proliferation or migration of these cells [9].

Src homology 2-containing protein tyrosine phosphatase 2 (Shp2, also known as PTPN11) is a cytoplasmic PTP that contains two tandem Src homology 2 (SH2) domains [10,11]. Shp2 is expressed in most mammalian cell types and is thought to bind



through its SH2 domains to the tyrosine-phosphorylated platelet-derived growth factor (PDGF) receptor as well as to tyrosine-phosphorylated docking proteins (such as insulin receptor substrates, signal regulatory protein  $\alpha$ , and Grb2-associated binder proteins) in response to cell stimulation with growth factors or to cell adhesion. Such binding is important both for activation of the PTP activity of Shp2 as well as for its recruitment to sites near the plasma membrane where potential substrates are located [10,11]. Although PTPs are generally considered to be negative regulators on the basis of their ability to oppose the effects of PTKs, biochemical and genetic analyses indicate that Shp2 is required for activation of the Ras–mitogen-activated protein kinase (MAPK) signaling pathway operative downstream of the receptors for various growth factors and cytokines, and that it thereby contributes to the promotion of cell proliferation, differentiation, or survival [10,11]. Moreover, Shp2 is also implicated in the regulation of cell adhesion and migration, in part through its control of the activity of the small GTP-binding protein Rho [12,13]. Indeed, homozygous Shp2 mutant mice were found to die as embryos as a result of a defect in gastrulation and abnormal mesoderm patterning [14].

The precise role of Shp2 in the regulation of IEC function, especially in vivo, has remained unclear, however. To address this issue, we have now generated and analyzed IEC-specific Shp2 conditional knockout (CKO) mice.

## Materials and Methods

### Ethics Statement

This study was approved by the Institutional Animal Care and Use Committee of Kobe University (Permit Number: P130206, P120304-R2, P110402), and all animal experiments were performed according to Kobe University Animal Experimentation Regulations. All efforts were made to minimize suffering.

### Antibodies and reagents

A mouse monoclonal antibody (mAb) to  $\beta$ -catenin was obtained from BD Biosciences (San Diego, CA), a mouse mAb to  $\beta$ -tubulin was from Sigma-Aldrich (St. Louis, MO), and a rat mAb to bromodeoxyuridine (BrdU) was from Abcam (Cambridge, MA). Rabbit polyclonal antibodies (pAbs) to Shp2 and to mucin 2 were obtained from Santa Cruz Biotechnology (Santa Cruz, CA), those to lysozyme were from Dako (Glostrup, Denmark), and those to cleaved caspase-3 (Asp<sup>175</sup>) were from Cell Signaling Technology (Danvers, MA). Alkaline phosphatase-conjugated sheep pAbs to digoxigenin for in situ hybridization were obtained from Roche (Basel, Switzerland). Cy3- or Alexa Fluor 488-conjugated goat secondary pAbs for immunofluorescence analysis were obtained from Jackson ImmunoResearch (West Grove, PA) and Invitrogen (Carlsbad, CA), respectively, and 4',6-diamino-2-phenylindole (DAPI) was from Nacalai Tesque (Kyoto, Japan). Horseradish peroxidase-conjugated goat secondary pAbs for immunoblot analysis were obtained from Jackson ImmunoResearch. Mayer's hemalum solution was from Merck KGaA (Darmstadt, Germany), and eosin was from Wako (Osaka, Japan).

### Mice

*Ptpn11*<sup>fl/fl</sup> mice were kindly provided by Dr. B. G. Neel (Princess Margaret Cancer Centre) [15]. The Rosa26 conditional reporter strain (*R26R*) of mice (B6.129S4-*Gt(ROSA)26Sor<sup>tm1Sor</sup>/J*) [16], *LSL-Kras G12D* mice (B6.129S4-*Kras<sup>tm4Tvj</sup>/J*) [17], and villin-*cre* mice (B6.SJL-Tg(Vil-*cre*)997Gum/J) [18] were obtained from Jackson Laboratory (Bar Harbor, ME). *R26R*;villin-*cre* mice were obtained by crossing *R26R* mice with villin-*cre* mice. To generate *Ptpn11*<sup>fl/+</sup>;

villin-*cre* mice, we crossed villin-*cre* mice with *Ptpn11*<sup>fl/fl</sup> mice. The resulting *Ptpn11*<sup>fl/+</sup>;villin-*cre* offspring were crossed with *Ptpn11*<sup>fl/fl</sup> mice to obtain *Ptpn11*<sup>fl/fl</sup>;villin-*cre* (Shp2 CKO) mice and *Ptpn11*<sup>fl/fl</sup> (control) mice. To generate *Ptpn11*<sup>fl/+</sup>;villin-*cre*;LSL-*Kras G12D* mice, we crossed Shp2 CKO mice with *LSL-Kras G12D* mice. The resulting *Ptpn11*<sup>fl/+</sup>;villin-*cre*;LSL-*Kras G12D* offspring were crossed with *Ptpn11*<sup>fl/fl</sup> mice to obtain *Ptpn11*<sup>fl/fl</sup>;villin-*cre*;LSL-*Kras G12D* (Shp2 CKO;LSL-*Kras G12D*) mice and Shp2 CKO mice. All mice were maintained in the Institute for Experimental Animals at Kobe University Graduate School of Medicine under specific pathogen-free conditions. The genotype of all offspring was determined by polymerase chain reaction (PCR) analysis.

### Detection of deleted and floxed alleles of *Ptpn11* by PCR

For preparation of genomic DNA, various tissues isolated from adult control or Shp2 CKO mice were washed with ice-cold phosphate-buffered saline (PBS), incubated overnight at 56°C in lysis buffer (100 mM Tris-HCl [pH 8.5], 5 mM EDTA, 0.2% SDS, 200 mM NaCl, proteinase K [50  $\mu$ g/ml]), and centrifuged at 17,500 $\times$ g for 15 min at 4°C. The resulting supernatant was subjected to isopropanol precipitation for separation of genomic DNA. The floxed *Ptpn11* allele (~400-bp product) was identified by PCR with the sense primer SHP2F (5'-TAGCTGCTT-TAACCCCTCTGTGT-3') and the antisense primer SHP2R (5'-CATCAGAGCAGGCCATATTCC-3'), whereas the deleted allele (~500-bp product) was identified with the sense primer SHP2F and the antisense primer SHP2R#3 (5'-TCACAAT-GAAGGTTCCCTGTCC-3').

### Isolation of mouse IECs

Mouse IECs were isolated as previously described [19] but with slight modifications. In brief, the freshly isolated whole intestine of adult control or Shp2 CKO mice was washed with PBS, cut into small pieces, washed three times with Hanks' balanced salt solution (HBSS) containing 1% fetal bovine serum and 25 mM HEPES-NaOH (pH 7.5), and then incubated three or four times on a rolling platform for 15 min at room temperature in HBSS containing 50 mM EDTA and 25 mM HEPES-NaOH (pH 7.5). The tissue debris was removed, and IECs in the resulting supernatant were isolated by centrifugation at 250 $\times$ g for 10 min at 4°C and washed three times with PBS.

### Immunoblot analysis

Isolated cells or tissues were washed with ice-cold PBS and then homogenized on ice in RIPA buffer (20 mM Tris-HCl [pH 7.5], 150 mM NaCl, 2 mM EDTA, 1% Nonidet P-40, 1% sodium deoxycholate, 0.1% SDS, 50 mM NaF) containing 1 mM sodium vanadate and a protease inhibitor cocktail (Nacalai Tesque). The lysates were centrifuged at 17,500 $\times$ g for 15 min at 4°C, and the resulting supernatants were subjected to immunoblot analysis as previously described [8,19].

### Assessment of colitis

For assessment of colitis, Shp2 CKO and control mice were weighed weekly and monitored for the appearance of diarrhea, blood in the stool, and anorectal prolapse. Disease activity was scored as previously described [20,21] with minor modifications. Stool consistency was scored as: 0 = normal, 2 = loose stools, 4 = liquid stools. Blood in the stool was scored as: 0 = no blood as revealed with the guaiac occult blood test (Occult Blood Slide II; Shionogi Pharmaceutical, Osaka, Japan), 2 = positive guaiac occult blood test, 4 = gross bleeding. Development of anorectal prolapse was scored as: 0 = no prolapse, 2 = prolapse evident only during

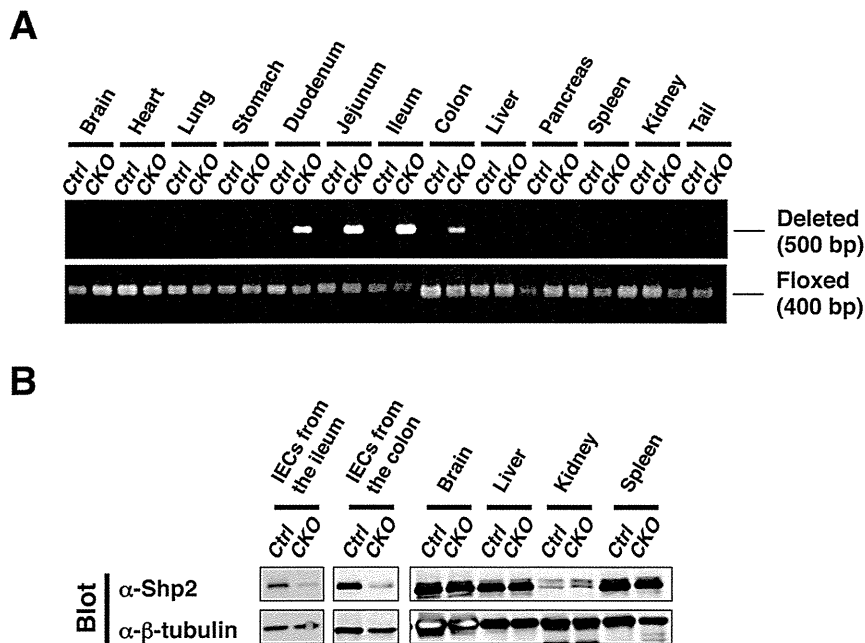


**Figure 1. Generation of IEC-specific Shp2 CKO mice.** **A:** Genomic DNA extracted from the indicated organs of adult control (Ctrl) or Shp2 CKO (CKO) mice was subjected to PCR analysis with primers specific for deleted or floxed alleles of *Ptpn11*. Data are representative of three separate experiments. **B:** Lysates of IECs (from the ileum or colon) and the indicated organs from control or Shp2 CKO mice were subjected to immunoblot analysis with antibodies to ( $\alpha$ -) both Shp2 and  $\beta$ -tubulin (loading control). Data are representative of three (IECs) or two (indicated organs) separate experiments.

doi:10.1371/journal.pone.0092904.g001

defecation, 4 = prolapse evident at all times. The total score for diarrhea, blood in the stool, and prolapse, ranging from 0 (normal) to 12 (severe), was determined as the disease activity index (DAI).

### Histology and immunofluorescence analysis

For histological analysis, the small intestine and colon were removed and immediately fixed for 3 h at room temperature with 4% paraformaldehyde in PBS. Paraffin-embedded sections (thickness of 5  $\mu$ m) were then prepared and stained with hematoxylin-eosin. For immunofluorescence analysis, the small intestine or colon was fixed as for histology and then transferred to a series of sucrose solutions (7, 20, and 30% [w/v], sequentially) in PBS for cryoprotection, embedded in OCT compound (Sakura, Tokyo, Japan), and rapidly frozen in liquid nitrogen. Frozen sections with a thickness of 5  $\mu$ m were prepared with a cryostat, mounted on glass slides, and air-dried. The sections were then subjected to immunofluorescence analysis with primary antibodies and fluorescent dye-labeled secondary antibodies as described previously [8]. Images were obtained with a fluorescence microscope (BX51; Olympus, Tokyo, Japan).

### $\beta$ -Galactosidase staining

Staining for  $\beta$ -galactosidase was performed as previously described [22] with slight modifications. In brief, the colon and small intestine were removed, fixed for 30 min at 4°C with 0.2% glutaraldehyde and 4% paraformaldehyde in PBS, and washed with PBS. The tissue was then transferred to a series of sucrose solutions (7, 20, and 30% [w/v], sequentially) in PBS, embedded in OCT compound, and rapidly frozen with liquid nitrogen. Frozen sections with a thickness of 10  $\mu$ m were prepared and then stained for 2 to 10 h at 37°C with  $\beta$ -galactosidase substrate (X-gal [1 mg/ml], 4 mM  $K_3Fe(CN)_6$ , 4 mM  $K_4Fe(CN)_6 \cdot 3H_2O$ , 2 mM

$MgCl_2$ ) in PBS. Stained sections were examined with a fluorescence microscope (BX51, Olympus).

### In situ hybridization

Expression of the Olfactomedin4 (*Olfm4*) gene in the intestinal epithelium was examined by in situ hybridization performed as described previously [23]. In brief, paraffin-embedded sections of the ileum (thickness of 10  $\mu$ m) were depleted of paraffin with xylene, rehydrated by exposure to a graded series of ethanol solutions, and treated with 0.2 M HCl and proteinase K. The sections were then fixed again with 4% paraformaldehyde, demethylated with acetic anhydride, and subjected to hybridization for 48 h at 65°C with a digoxigenin-labeled RNA probe for *Olfm4* mRNA (IMAGE clone 1078130) at 500 ng/ml. They were then incubated overnight at 4°C with alkaline phosphatase-conjugated pAbs to digoxigenin, washed, and incubated with nitro blue tetrazolium chloride and 5-bromo-4-chloro-3-indolyl phosphate (Sigma-Aldrich). Images were obtained with a fluorescence microscope (BX51, Olympus).

### BrdU incorporation assay

Mice were injected intraperitoneally with BrdU (50 mg/kg) and killed 2 or 48 h later. The ileum or colon was fixed with 4% paraformaldehyde, transferred to a series of sucrose solutions in PBS, embedded in OCT compound, and rapidly frozen with liquid nitrogen as described for immunofluorescence analysis. Sections with a thickness of 5  $\mu$ m were incubated for 30 min at 65°C with 0.025 M HCl, washed with 0.1 M borate buffer (pH 8.5), and incubated at room temperature first for 2 h with mAbs to BrdU and to  $\beta$ -catenin and then for 1 h at room temperature with fluorescent dye-labeled secondary pAbs. Fluorescence images were obtained with a fluorescence microscope (BX51, Olympus). IEC migration distance was defined as the distance from the crypt